




ORIGINAL ARTICLE

Neutron diffraction study of antibacterial bioactive calcium silicate sol-gel glasses containing silver

Daniela Carta^{1,2}  | Julian R. Jones³  | Sen Lin³ | Gowsihan Poologasundarampillai³ | Robert J. Newport²  | David M. Pickup²

¹Department of Chemistry, University of Surrey, Guildford, UK

²School of Physical Sciences, Ingram Building, University of Kent, Canterbury, UK

³Department of Materials, Imperial College London, London, UK

Correspondence

Daniela Carta
Email: d.carta@surrey.ac.uk

Funding information

EPSRC funded National Chemical Database Service, Grant/Award Number: GR/88595/01; Royal Society of Chemistry

Abstract

Bioactive sol-gel calcia-silica glasses can regenerate damaged or diseased bones due to their ability to stimulate bone growth. This capability is related to the formation of a hydroxyapatite layer on the glass surface, which bonds with bone, and the release of soluble silica and calcium ions in the body fluid which accelerates bone growth. The addition of silver ions imbues the glass with antibacterial properties due to the release of antibacterial Ag^+ ion. The antibacterial activity is therefore closely dependent on the dissolution properties of the glasses which in turn are related to their atomic-level structure. Structural characterization of the glasses at the atomic level is therefore essential in order to investigate and control the antibacterial properties of the glass. We have used neutron diffraction to investigate the structure of silver-containing calcia-silica sol-gel bioactive glasses with different Ag_2O loading (0, 2, 4, 6 mol%). The presence of the silver had little effect on the host glass structure, although some silver metal nanoparticles were present. Results agreed with previous computer simulations.

KEYWORDS

bioglass, calcium silicate glasses, Glass Forming Systems, neutron diffraction, silicate, Sol-gel

1 | INTRODUCTION

Glasses based on a silicate network with the addition of CaO as modifier oxide are used within biomedical research as synthetic bone grafts for orthopedic and dental applications.¹ Of particular interest is the commercially available Bioglass[®], developed by Hench et al,^{2,3} which is based on a melt-derived silicate glass network containing CaO, Na_2O and P_2O_5 . In particular, the original Bioglass[®], 45S5, containing 46.1 mol% SiO_2 and having 5:1 molar ratio of calcium to phosphorus is particularly effective in regenerating damaged tissues. When Bioglass[®] is immersed in aqueous media, including body fluid, it undergoes dissolution,

generating a bone-like layer of carbonated hydroxyapatite that strongly bonds to bone.^{2,4} However, all implants have the risk of post-surgery problems arising from bacterial adhesion to the implant that can later cause infection.⁴ Administration of antibiotics to tackle bacterial infection is not desirable with the increase in resistance to them due to overuse. The efficacy of antibiotics is also reduced in the presence of biomaterial-adherent strains.⁵ Introduction of Ag_2O in SiO_2 -CaO glasses reduces the risk of bacterial infection due to the antimicrobial action of the leaching Ag^+ .^{4,6} Silver has a broad-spectrum antimicrobial action, which is particularly important when dealing with polymicrobial colonizations associated with biomaterial-centered infections.^{6,7} The

glasses presented in this work were made using the sol-gel process. The conventional method to prepare silicate glasses is melt quenching, which consists of bringing the solid precursors to temperatures $>1000^{\circ}\text{C}$. The sol-gel process is a wet chemical bottom-up technique based on the hydrolysis and polycondensation of precursors in solution,^{8–10} which is more versatile than the melt-quenching technique, allowing one to extend the compositional range over which glasses can be prepared. Gels can be shaped at room temperature, in many forms (monoliths, porous foam scaffolds, fibres, monodispersed spherical nanoparticles, thin films)^{11–14} and then dried and thermally stabilized, reducing loss of volatile composition components (eg Li).^{15,16} Sol-gel glasses show higher degradation rates compared to melt-derived glasses of similar nominal composition; this is due their nanoporosity and due to their network connectivity being lower than theoretical because of residual H^+ ions acting as network modifiers.^{17–19} The nanoporous glass matrix that is inherent to the sol-gel process facilitates a controlled, sustained delivery of the antibacterial agent Ag^+ .^{6,20} Incorporation of 3 wt% Ag_2O into bioactive calcium silicate sol-gel glass imparted potent antibacterial activity without compromising bioactivity.⁶ The significant bactericidal effect of silver-containing calcium silicate-based sol-gel glasses was demonstrated on *E. coli*, *Pseudomonas aeruginosa*, and *Staphylococcus aureus*.^{4,6,20–23} In vitro studies have shown that primary human osteoblasts attach, grow and proliferate on the surface of the silver containing glasses.²⁴ This indicates that the presence of silver does not affect the bioactivity of the material. As the bioactivity and the antibacterial action of the glasses are, respectively, related to the release of Ca^{2+} and Ag^+ ions that are incorporated in the glass network, a quantitative knowledge of the glass structure at the atomic level, in particular to the way the modifier cations are connected to and modify the structure of the main network, is of paramount importance. Neutron diffraction has previously proven to be a successful tool for the investigation of SiO_2 - CaO -based bioactive sol-gel glasses.^{25–27} Here, the aim was to use neutron diffraction to investigate the atomic structure of bioactive SiO_2 - CaO sol-gel glasses with SiO_2 as the main component (~ 70 mol%), and with Ag_2O incorporated at a relatively low level (2–6 mol%). Neutron diffraction allows us to investigate the structure of such ternary oxide glasses by resolving the important correlations between atoms, ie the Si–O, Ca–O, Ag–O distances, along with their coordination numbers.

2 | EXPERIMENTAL

2.1 | Sample preparation

All reagents were purchased from Sigma-Aldrich (UK). Glasses were synthesized of the following compositions: 70 mol% SiO_2 , $30-x$ mol% CaO , x mol% Ag_2O , where

$x = 0, 2, 4, 6$.^{4,11} Synthesis was performed in a darkened room with covered beakers to prevent the reduction in silver nitrate or silver oxide precursors to silver metal. A sol was produced by the hydrolysis of TEOS (tetraethoxysilane), using a water:TEOS molar ratio of 12 and using 2 N HNO_3 (1 mL per 6 mL of H_2O). After hydrolysis was completed (1 hours stirring), calcium nitrate tetrahydrate was added and allowed to mix for 1 hours. Then silver nitrate was added and stirring performed for 1 hours. The sols were poured into screw-top cylindrical polymethyl pentene moulds and sealed. They were left to gel (polycondensation) at room temperature for 3 days and then aged for 3 days at 60°C . The screw tops were unscrewed to the final thread and then dried at 130°C (heating rate $1^{\circ}\text{C}/\text{min}$). The dried gels were then removed from their moulds and placed on a refractory surface in a furnace, where they were heated to 600°C (heating rate $1^{\circ}\text{C}/\text{min}$), holding for 3 hours. The 70 mol% SiO_2 , 28 mol% CaO , 2 mol% Ag_2O glass was additionally heated to 800°C at $1^{\circ}\text{C}/\text{min}$ and held for 2 hours before allowing the furnace to cool to room temperature. The sample containing 2 mol% of Ag_2O was further annealed at 800°C because it was previously shown that Ag^+ release from calcium silicate glasses treated at 600°C was rapid during the first hour of immersion in simulated body fluid (SBF)¹¹ and sintering at 800°C made the material more suitable by reducing the Ag^+ release rate and by improving the mechanical properties.^{11,28} All glasses were stored in darkened containers. A list of the samples is reported in Table 1.

2.2 | Neutron scattering

The neutron diffraction data were collected on the GEM diffractometer on the ISIS spallation neutron source at the Rutherford Appleton Laboratory, UK. The finely powdered samples were held in 8 mm diameter vanadium foil cans, which have a very low cross section for the coherent scattering of neutrons, and time-of-flight data collected over a wide range of Q (where $Q = 4\pi\sin\theta/\lambda$, where 2θ is the scattering angle). We performed the neutron diffraction experiment using a $Q_{\text{max}} \sim 40 \text{ \AA}^{-1}$ which provides a

TABLE 1 Nominal glasses compositions and heat treatment temperatures

Sample	SiO_2 (mol%)	CaO (mol%)	Ag_2O (mol%)	Heat treatment ($^{\circ}\text{C}$)
Si70Ca30_600	70	30	0	600
Si70Ca28Ag2_600	70	28	2	600
Si70Ca28Ag2_800	70	28	2	800
Si70Ca26Ag4_600	70	26	4	600
Si70Ca24Ag6_600	70	24	6	600

sufficiently good real-space resolution of the Ag–O pair distance to enable the required detailed study. The program GUDRUN was used to reduce and correct the data.²⁹ The initial stages of analysis of neutron scattering data were the removal of background scattering, normalization, correction for absorption, inelastic and multiple scattering and subtraction of the self-scattering term.^{29,30} In this case, since sol-gel glasses have a high surface area which is populated with hydroxyl groups, it was necessary to correct for the effect of inelastic scattering associated with hydrogen by approximating the self-scattering with Chebyshev polynomials fitted to the data.³¹ The resultant total scattering structure factors, $S(Q)-1$, were Fourier transformed to obtain pair distribution functions:

$$T(r) = T^0(r) + 2/\pi \int_0^\infty Q(S(Q) - 1)M(Q)\sin(Qr)dQ \quad (1)$$

where $T^0(r) = 4\pi r\rho_0$ (r is the atomic separation and ρ_0 the macroscopic number density) and $M(Q)$ is a Fourier transformation window function necessitated by the finite maximum experimentally attainable value of Q . Structural information (coordination number N , atomic separation R and disorder parameter σ) was obtained from the pair distribution functions by simulation, using the program NXFit.³⁰ Uncertainties were estimated by processing the same dataset multiple times with different starting parameters; a small additional estimated uncertainty has been included in N because sol-gel samples can change composition over time either taking up or losing H_2O depending on conditions and making it almost impossible to know composition with the same level of precision one might associate with a melt-quenched glass. Furthermore, it is

recognized that the empirical correction for H incoherent scattering introduces further uncertainty. For the Ag–O and Ca–O correlations, the estimated uncertainties are $\pm 0.04 \text{ \AA}$ in R , $\pm 20\%$ in N and $\pm 25\%$ in σ . For all other correlations they are $\pm 0.01 \text{ \AA}$ in R , $\pm 15\%$ in N and $\pm 10\%$ in σ .

2.3 | High-resolution transmission electron microscopy (HRTEM)

HRTEM and electron diffraction were performed on JEM-2010 (JEOL, UK). The sample was prepared by manually grinding to a fine powder and mixing in acetone to create a suspension. The TEM grid was dipped in the suspension and air-dried before analysis.

3 | RESULTS AND DISCUSSION

Figure 1A shows the total scattering structure factors, $S(Q)-1$, from the silver-doped sol-gel bioactive glasses, along with data from a $(SiO_2)_{0.7}(CaO)_{0.3}$ sol-gel glass containing no silver for comparison. Figure 1B shows the real-space pair distribution functions, $T(r)$, obtained by Fourier transformation of the curves shown in Figure 1A.

The $S(Q)-1$ from the 2 mol% Ag_2O sample heated to $800^\circ C$ exhibits Bragg peaks, indicating that it was partially crystalline. The Bragg peaks can be indexed to pseudowollastonite, $Ca_3(Si_3O_9)$, Inorganic Crystal Structure Database (ICSD) entry number 26553.³² Neutron real-space pair distribution functions, $T(r)$ were then fitted in order to obtain details of the glass structure. Examples of typical fits to the $T(r)$ functions together with the key correlations that comprise the fits are shown in Figure 2. The structural

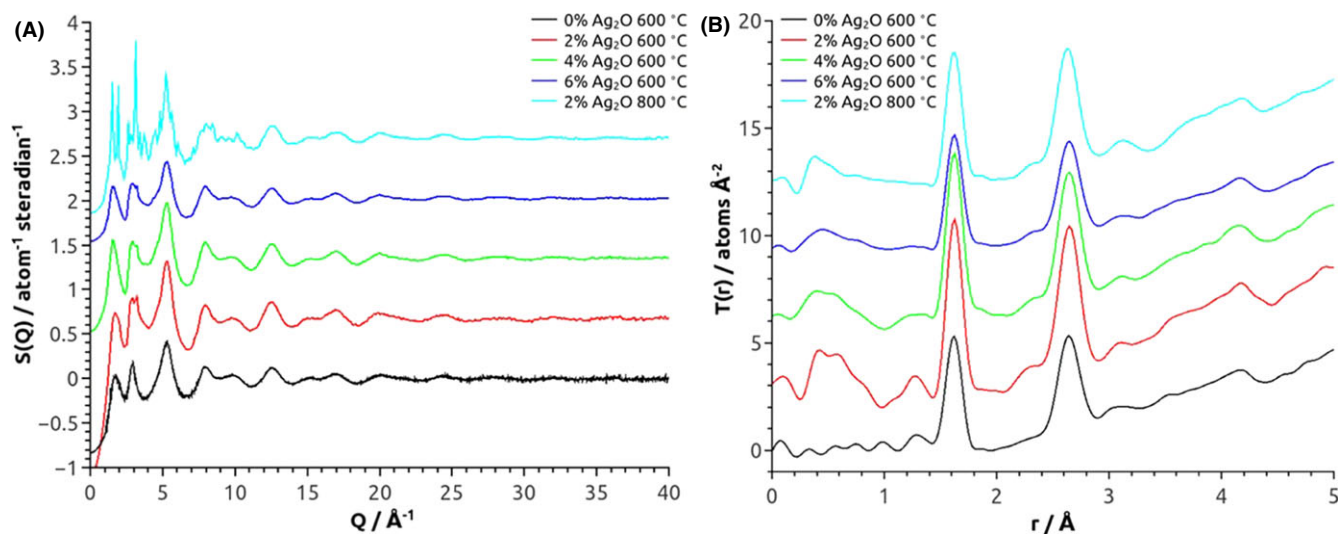


FIGURE 1 A, Neutron total scattering structure factors, $S(Q)-1$ and B, neutron real-space pair distribution functions, $T(r)$ from Ag-doped calcium silicate sol-gel glasses (plots are in reverse order to the legend) [Color figure can be viewed at wileyonlinelibrary.com]

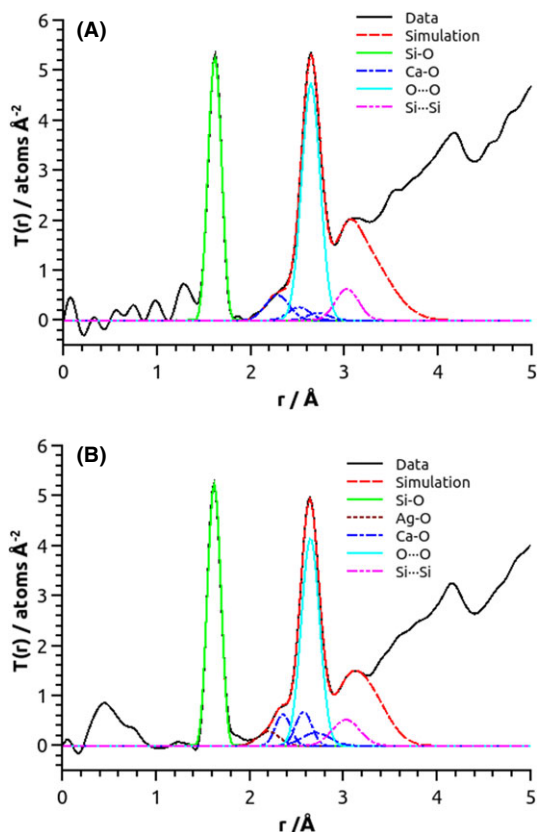


FIGURE 2 Typical fits to the neutron real-space pair distribution functions showing the main partial correlation functions that comprise the fit. A, Si70Ca30_600 and B, Si70Ca24Ag6_600 [Color figure can be viewed at wileyonlinelibrary.com]

parameters obtained from the simulations of the $T(r)$ functions are reported in Table 2. The results in Table 2 show that in all samples the silicon is surrounded by oxygens at a distance of 1.61–1.62 Å with a coordination numbers in the range 3.3–4.4. Although imprecise, this is nevertheless consistent with the presence of SiO_4 tetrahedra anticipated within the structure of silicate-based glasses.^{33,34} The measured O...O and Si...Si distances of ~ 2.64 and ~ 3.03 Å, respectively, are those expected in a network of corner-sharing SiO_4 tetrahedra.³⁴ It is noted that the Si–O coordination numbers have a wider distribution compared to the conventional prepared melt quenched glasses.^{35,36} This could be explained with the fact that, due to their high surface area, these materials are prone to absorb moisture. Therefore, it is relatively difficult to offer precise values for the O and H content. This content could also change with aging of the glass and during the neutron diffraction experiment itself, which is performed under high vacuum. However, it remains the case that the variation in these first-shell coordination numbers is higher than would be expected even for a sol-gel derived material and one might therefore speculate that changes to the O and H content are more severe in this case.

In all samples, three Ca–O distances can be discerned at ~ 2.3 , 2.5–2.6 and 2.7–2.8 Å. The presence of three Ca–O distances and their lengths are in good agreement with the results of the neutron diffraction with isotopic substitution study of $(\text{SiO}_2)_{0.7}(\text{CaO})_{0.3}$ sol-gel glass²⁵ and with an molecular dynamics (MD) modeling study by Mead and Mountjoy.³⁷ The silver containing glasses all exhibit an Ag–O distance in the range 2.18–2.25 Å with a coordination number in the range 1.3–2.1. Structural studies of the environment of silver in silicate glasses are quite rare. However, there is an Extended X-Ray Absorption Fine Structure (EXAFS) study that provides evidence of the type of environment that the Ag^+ ions can adopt³⁸ wherein the silver environment in sodium silicate and alumina silicate ion-exchange glasses with varying silver contents was probed. The results revealed average Ag–O distances of 2.08, 2.11, and 2.23 Å for a sodium silicate glass containing <1 mol% Ag, an alumino silicate glass containing ~ 1 mol% and an alumino silicate glasses containing ~ 17 mol% silver, respectively. The respective silver coordination numbers (with respect to oxygen) in these three glasses were 2.1, 1.8 and 2.5. The samples studied here contain between 2 and 6 mol% Ag_2O so silver is by far the minority component of the glasses and consequently the uncertainties associated with the parameters for the Ag–O correlations in Table 2 (± 0.04 Å in R, $\pm 20\%$ in N and $\pm 25\%$ in σ) are significant. Nonetheless, the average Ag–O distance and coordination number of 2.21 Å and 1.7, respectively, determined with neutron diffraction are in broad agreement with those determined from EXAFS³⁸ if the uncertainties associated with the respective measurements are taken into account. We cannot rule out the presence of longer Ag–O correlations similar to those at ~ 2.5 and 2.7 Å observed in silver phosphate glasses, using neutron diffraction with isotopic substitution (NDIS) by Moss et al.³⁹ In this case, such correlations would be impossible to observe in the pair distributions functions because they would be masked by the much stronger Ca–O and O...O correlations. No significant variation in silver environment with content was observed in the samples. The low Ag–O coordination number may possibly be due to the formation of Ag nanoparticles embedded in the glass matrix. The HRTEM image of the Si70Ca28Ag2 glass calcined at 700°C reported in Figure 3, does indicate the presence of spherical nanoparticles with a diameter of about 8 nm. The electron diffraction (ED) pattern reported in the inset of Figure 3 confirms that the nanoparticles are formed by metallic silver as the rings observed correspond to the planes (111), (200), (220) and (311). Low Ag–O correlation numbers in the range 1.3–1.6 have previously been reported in silicate glasses containing Ag nanoparticles.^{38,40} A short Ag–O correlation at 2.28 Å with a coordination number of 2.1 was also observed in Ag-doped phosphate

TABLE 2 Structural parameters obtained from the simulation of the T(r) functions

Sample	Heat treatment (°C)	Correlation	R (Å)	N (atoms)	σ (Å)
Si70Ca30	600	Si-O	1.61	3.5	0.05
		Ca-O	2.28	3.4	0.12
		Ca-O	2.51	1.8	0.11
		O...O	2.64	4.0	0.09
		Ca-O	2.72	1.1	0.11
		Si...Si	3.03	3.9	0.11
Si70Ca28Ag2	600	Si-O	1.62	3.7	0.04
		Ag-O	2.25	1.6	0.06
		Ca-O	2.32	1.2	0.06
		Ca-O	2.52	1.9	0.10
		O...O	2.64	4.1	0.08
		Ca-O	2.77	1.6	0.07
		Si...Si	3.04	3.3	0.11
Si70Ca26Ag4	600	Si-O	1.62	4.4	0.05
		Ag-O	2.20	1.3	0.13
		Ca-O	2.33	1.7	0.06
		Ca-O	2.58	2.3	0.07
		O...O	2.64	4.1	0.09
		Ca-O	2.68	1.9	0.09
		Si...Si	3.03	3.6	0.16
Si70Ca24Ag6	600	Si-O	1.62	3.3	0.05
		Ag-O	2.19	1.7	0.10
		Ca-O	2.35	1.7	0.06
		Ca-O	2.57	2.1	0.07
		O...O	2.65	3.5	0.09
		Ca-O	2.70	1.5	0.14
		Si...Si	3.02	3.6	0.14
Si70Ca28Ag2	800	Si-O	1.62	3.6	0.04
		Ag-O	2.18	2.1	0.14
		Ca-O	2.34	1.9	0.07
		Ca-O	2.58	2.1	0.06
		O...O	2.63	4.2	0.08
		Ca-O	2.75	2.2	0.11
		Si...Si	3.06	3.5	0.14

based glasses.³⁹ In terms of the application, silver nanoparticles have been used as nanoparticles⁴¹ and as coatings for titanium implants in order to inhibit bacterial colonization.⁴²

An important parameter used to describe the connectivity of silica based glasses is the Q-speciation, where Qⁿ represents an SiO₄ tetrahedral unit that is bonded to n other such units by corner sharing. The relative proportions of

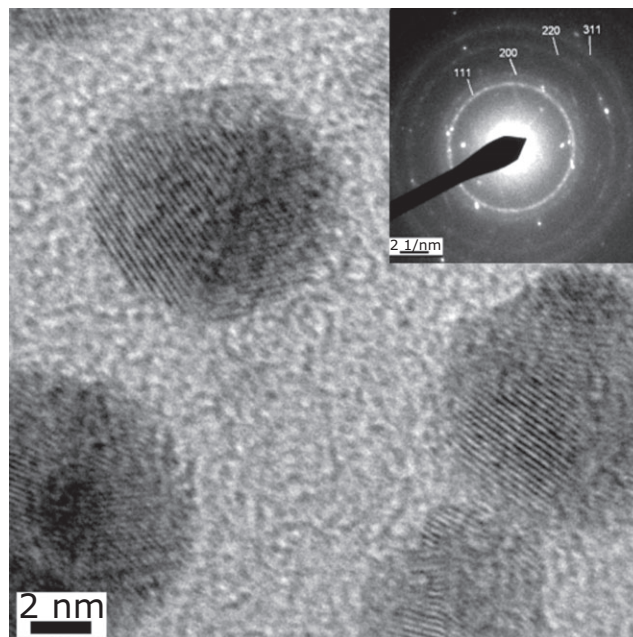


FIGURE 3 High-resolution TEM image of Si70Ca28Ag2 calcined at 700°C. Inset: electron diffraction pattern showing the (111), (200), (220) and (311) reflections of silver

the various Qⁿ species (ranging from Q⁰ to Qⁿ) that form the silica network in a glass are often determined by²⁹ Si NMR.⁴³ However, the average Q-species, \bar{Q}^n , can also be obtained from diffraction data because \bar{Q}^n is equal to the average Si...Si coordination number. The glasses studied here all have Si...Si coordination numbers of between 3.3 and 3.9 and exhibit no clear systematic variation with silver content. The Si...Si coordination numbers reported here are consistent with those in the literature: Lin and co-workers reported values of 3.6 and 3.7 for \bar{Q}^n measured from different regions of (SiO₂)_{0.7}(CaO)_{0.3} sol-gel glass monoliths.⁴⁴ The experimental \bar{Q}^n can be compared with that calculated from the composition of the glasses (\bar{Q}_T^n). If we assume that all of the oxygen is bonded to at least one silicon atom, the average Q-species can be estimated, using the following equation:

$$\bar{Q}_T^n = 2(4 - O/Si)$$

where O/Si is the mole ratio of O to Si from the nominal composition. The glasses studied here all have a nominal O/Si ratio of 2.4 which would give a \bar{Q}_T^n of 3.2. This is lower than the average experimental value of 3.6, which reflects the network modifying effects of the H content and the consequential fact that not all the oxygen present in the sample contributes to the silica network. However, this does not affect the theoretical Si-O and Si...Si coordination numbers. A similar discrepancy was observed in MD models of (SiO₂)_{1-x}(CaO)_x sol-gel materials,³⁷ and was attributed to a proportion of the oxygen being shared between calcium ions or present in Ca-OH groups and not bonded

to silicon. The results presented here thus provide experimental evidence that validates the MD models of Mead and Mountjoy.³⁷ Furthermore, the presence of oxygen shared between calcium ions means that a degree of calcium clustering cannot be ruled out. It is well known that silver ions in silicate-based sol-gel glasses can be reduced to silver metal, often in the form of nanoparticles, during the materials' processing.⁴⁵ Delben et al.⁴⁶ found Bragg peaks due to metallic silver in X-ray diffraction (XRD) patterns from their silver-doped 45S5 Bioglass. Using data from the ICSD (entry no. 181730), the expected positions of the Bragg peaks due to metallic silver in Q-space can be calculated. Using the crystallographic data from reference,⁴⁷ Bragg peaks due to metallic silver are expected to be at 2.7, 3.1, 4.5 and 5.1 Å⁻¹ in Q-space. Examining the neutron pair distribution functions in Figure 1B, we see no evidence of Bragg peaks at these positions, with the exception of the peak at 3.1 Å⁻¹, particularly evident in the 2 mol% Ag₂O containing sample heated to the higher temperature of 800°C that can be attributed to pseudowollastonite.³² Even though Ag nanoparticles are present in the sample after calcination at 700°C (Figure 3), no peaks corresponding to metallic silver are observed in Figure 1A. This may be due to the small dimensions of the nanoparticles, which makes the peaks very broad and difficult to distinguish, and also to the low concentration of silver in the glass matrix. Previous XRD studies on the silver-free (SiO₂)_{0.7}(CaO)_{0.3} composition detected no crystallization at 800°C but did find pseudowollastonite peaks at 850°C (no patterns were collected between 800°C and 850°C).⁴⁸ The results of the neutron diffraction study presented here suggest that substituting some calcium for silver in sol-gel (SiO₂)_{0.7}(CaO)_{0.3} bioactive glass up to a level of 6 mol% had no significant effect on the structure, for samples heat treated at 600°C. Heat treatment of the 2 mol% Ag₂O sample to 800°C resulted in some crystallization of pseudowollastonite, Ca₃(Si₃O₉). Furthermore, the results suggest that Ag⁺ ions (ie the silver not residing within metallic nanoparticles) are distributed throughout the silica network and are coordinated to ~2 oxygen atoms at a distance of 2.2 Å. The results of this structural study are entirely consistent with properties exhibited by the material; the bioactivity of the glasses is maintained because the structure is not disrupted by the addition of Ag₂O, whilst the presence of Ag⁺ ions which are coordinated by oxygen and slowly released as the glass dissolves imparts potent antibacterial qualities.

4 | CONCLUSIONS

This neutron diffraction study suggests that the addition of silver does not significantly modify the SiO₂-CaO glass

structure. The silver environment is consistent with that in silver-containing sodium silicate and alumina silicate glasses determined, using EXAFS. This result suggests that the silver is incorporated into and throughout the glass structure rather than existing in isolated regions of Ag₂O. However, some Ag nanoparticles were present, resulting in the observed low Ag-O coordination numbers. The average Q-speciation, calculated from the Si...Si coordination numbers, is similar for all samples and consistent with that measured with²⁹ Si NMR. This conclusion is in agreement with a previous molecular dynamics study, and with the conclusion that some oxygen atoms are likely to be shared between calcium ions or to be present within hydroxyl groups. All samples are mainly amorphous after heat treatment at 600°C. Further heat treatment of the sample, containing 2 mol% Ag₂O sample to 800°C caused partial crystallization to pseudowollastonite.

ACKNOWLEDGMENTS

We acknowledge the use of the EPSRC funded National Chemical Database Service hosted by the Royal Society of Chemistry, the EPSRC funded studentship GR/88595/01 and the assistance of Dr Alex Hannon during the collection of the neutron data.

ORCID

Daniela Carta  <http://orcid.org/0000-0002-4344-4061>
Julian R. Jones  <http://orcid.org/0000-0002-2647-8024>
Robert J. Newport  <https://orcid.org/0000-0002-2365-992X>

REFERENCES

1. Jones JR, Brauer DS, Hupa L, Greenspan DC. Bioglass and bioactive glasses and their impact on healthcare. *Int J Appl Glas Sci.* 2016;7:423-434.
2. Hench LL, Splinter RJ, Allen WC, Greenlee TK. Bonding mechanisms at the interface of ceramic prosthetic materials. *J Biomed Mater Res A.* 1971;5:117-141.
3. Hench LL, Jones JR. Bioactive Glasses: Frontiers and Challenges. *Front Bioeng Biotechnol.* 2015;3:1-12.
4. Bellantone M, Coleman NJ, Hench LL. Bacteriostatic action of a novel four-component bioactive glass. *J Biomed Mater Res.* 2000;51:484-490.
5. Naylor P, Myrvik Q, Gristina AG. Antibiotic Resistance of Biomaterial-Adherent Coagulase-Negative and Coagulase-Positive Staphylococci. *Clin Othopaedics Relat Res.* 1990;261:126-133.
6. Bellantone M, Williams HD, Hench LL. Broad-Spectrum Bactericidal Activity of Ag₂O-Doped Bioactive Glass. *Antimicrob Agents Chemother.* 2002;46:1940-1945.
7. Gristina AG. Biomaterial-centered infection: microbial adhesion versus tissue integration. *Science.* 1987;80:1588-1595.

8. Hench LL. Opening paper 2015-Some comments on Bioglass: Four Eras of Discovery and Development. *Biomed Glasses*. 2015;1:1-11.
9. Owens GJ, Singh RK, Foroutan F, et al. Sol-gel based materials for biomedical applications. *Prog Mater Sci*. 2016;77:1-79.
10. Hench LL, West JK. The sol-gel process. *Chem Rev*. 1990;90:33-72.
11. Jones JR, Ehrenfried LM, Saravanapavan P, Hench LL. Controlling ion release from bioactive glass foam scaffolds with antibacterial properties. *J Mater Sci Mater Med* 2006;17:989-996.
12. Poologasundarampillai G, Lam C, Kourkouta AM, Lee PD, Jones JR. Compressive strength of bioactive sol-gel glass foam scaffolds. *Int J Appl Glas Sci*. 2016;7:229-237.
13. Poologasundarampillai G, Wang D, Li S, et al. Cotton-wool-like bioactive glasses for bone regeneration. *Acta Biomater*. 2014;10:3733-3746.
14. Greasley SL, Page SJ, Sirovica S, et al. Controlling particle size in the Stöber process and incorporation of calcium. *J Colloid Interface Sci* 2016;469:213-223.
15. Maçon ALB, Jacquemin M, Jones JR. Lithium silicate sol-gel bioactive glass and the effect of lithium precursor on structure-property relationships. *J Sol-gel Sci Techn*. 2017;81:84-94.
16. Miguez VP, Büttner T, Maçon ALB, et al. Development and characterization of lithium-releasing silicate bioactive glasses and their scaffolds for bone repair. *J Non Cryst Solids*. 2016;432:65-72.
17. Sepulveda P, Jones JR, Hench LL. In vitro dissolution of mel-derived 45S5 and sol-gel derived 58S bioactive glasses. *J Biomed Mater Res*. 2002;61:301-311.
18. Jones JR. A review of bioactive glass - from Hench to Hybrids. *Acta Biomater*. 2013;9:4457-4486.
19. Lin Z, Jones JR, Hanna JV, Smith ME. A multinuclear solid state NMR spectroscopic study of the structural evolution of disordered calcium silicate sol-gel biomaterials. *Phys Chem Chem Phys*. 2015;17:2540-2549.
20. Catauro M, Bollino F, Papale F., Vecchio Cipriotti S. Investigation on bioactivity, biocompatibility, thermal behavior and antibacterial properties of calcium silicate glass coatings containing Ag. *J Non Cryst Solids*. 2015;422:16-22.
21. Kaur K, Singh KJ, Anand V, et al. Magnesium and silver doped CaO-Na₂O-SiO₂-P₂O₅ bioceramic nanoparticles as implant materials. *Ceram Int*. 2016;42:12651-12662.
22. Miola M, Verné E, Vitale-Brovarone C, Baino F. Antibacterial Bioglass-Derived Scaffolds: Innovative Synthesis Approach and Characterization. *Int J Appl Glas Sci* 2016;7:238-247.
23. Ni S, Li X, Yang P, et al. Enhanced apatite-forming ability and antibacterial activity of porous anodic alumina embedded with CaO-SiO₂-Ag₂O bioactive materials. *Mater Sci Eng, C*. 2016;58:700-708.
24. Saravanapavan P, Gough JE, Jones JR, Hench LL. Antimicrobial macroporous gel-glasses: dissolution and cytotoxicity. *Key Eng Mater*. 2004;254:1087-1090.
25. Skipper LJ, Sowrey FE, Pickup DM, et al. The structure of a bioactive calcia-silica sol-gel glass. *J Mater Chem*. 2005;15:2369-2374.
26. Newport RJ, Skipper LJ, FitzGerald V, Pickup DM, Smith ME, Jones JR. In vitro changes in the structure of a bioactive calcia-silica sol-gel glass explored using isotopic substitution in neutron diffraction. *J Non Cryst Solids*. 2007;353:1854-1859.
27. Martin RA, Moss RM, Lakhkar NJ, et al. Structural characterization of titanium-doped Bioglass using isotopic substitution neutron diffraction. *Phys Chem Chem Phys*. 2012;14:15807-15815.
28. Lohbauer U, Jell G, Saravanapavan P, et al. Indirect cytotoxicity evaluation of silver doped bioglass Ag-S70C30 on human primary keratinocytes. *Key Eng Mater*. 2005;284-286:431-434.
29. Hannon CA. Results on disordered materials from the General Materials diffractometer, GEM, at ISIS. *Nucl Instruments Methods Phys Res*. 2005;551:88-107.
30. Pickup DM, Moss RM, Newport RJ. NXFit: a program for simultaneously fitting X-ray and neutron diffraction pair distribution functions to provide optimized structural parameters. *J Appl Crystallogr*. 2014;47:1790-1796.
31. Johnson JA, Saboungi ML, Price DL, et al. Atomic structure of solid and liquid polyethylene oxide. *J Chem Phys*. 1998;109:7005-7010.
32. Yamanaka T, Hiroshi M. The Structure and Polytypes of α -CaSiO₃ (Pseudowollastonite). *Acta Crystallogr B*. 1981;37:1010-1017.
33. Lorch E. Neutron diffraction by germania, silica and radiation-damaged silica glasses. *J Phys Solid State Phys*. 1969;2:229-237.
34. Wright AC. Neutron scattering from vitreous silica: what have we learned from 60 years of diffraction studies. *J Non Cryst Solids*. 1994;179:84-115.
35. Martin RA, Twyman HL, Rees GJ, et al. An examination of the calcium and strontium site distribution in bioactive glasses through isomorphous neutron diffraction, X-ray diffraction, EXAFS and multinuclear solid state NMR. *J Mater Chem*. 2012;22:22212-22223.
36. Martin RA, Twyman HL, Rees GJ, et al. A structural investigation of the alkali metal site distribution within bioactive glass using neutron diffraction and multinuclear solid state NMR. *Phys Chem Chem Phys*. 2012;14:12105-12113.
37. Mead RN, Mountjoy G. Modelling the Local Atomic Structure of Bioactive Sol-Gel-derived Calcium Silicates. *Chem Mater*. 2006;18:3956-3964.
38. Houde-Walter SN, Inman JM, Dent AJ, Greaves GN. Sodium and Silver Environments and Ion-Exchange Processes in Silicate and Aluminosilicate Glasses. *J Phys Chem*. 1993;97:9330-9336.
39. Moss RB, Pickup DM, Ahmed I, Knowles JC, Smith ME, Newport RJ. Structural characteristics of antibacterial bioresorbable phosphate glass. *Adv Funct Mater*. 2008;18:634-639.
40. Yang XC, Li WJ, Dubiel M, Huang WH, Yano T. Silver structure environments in ion-exchanged silicate glasses studied by X-ray absorption fine structure. *J Nanosci Nanotechnol*. 2009;9:1659-1662.
41. Ramalingam B, Parandhaman T, Das SK. Antibacterial effects on biosynthesized silver nanoparticles on surface ultrastructure and nanomechanical properties of gram-negative bacteria viz. *Escherichia coli* and *Pseudomonas aeruginosa*. *ACS Appl Mater Interfaces*. 2016;8:4963-4976.
42. Devlin-Mullin A, Todd NM, Golrokhi Z, et al. Atomic layer deposition of a silver nanolayer on advanced titanium orthopedic implants inhibits bacterial colonization and supports vascularized de novo bone ingrowth. *Adv Healthc Mater*. 2017;6:1-14.
43. Stebbins JF. Effects of temperature and composition on silicate glass structure and dynamics: SI-29 NMR results. *J Non Cryst Solids*. 1988;106:359-369.

44. Lin S, Ionescu C, Baker S, Smith ME, Jones JR. Characterisation of the inhomogeneity of sol-gel-derived SiO₂-CaO bioactive glass and a strategy for its improvement. *J Sol-Gel Sci Technol.* 2010;53:255-262.
45. Kawashita M, Tsuneyama S, Miyaji F, Kokubo T, Kozuka H, Yamamoto K. Antibacterial silver-containing silica glass prepared by sol-gel method. *Biomaterials.* 2000;21:393-398.
46. Delben JR, Pimentel OM, Coelho MB, et al. Synthesis and thermal properties of nanoparticles of bioactive glasses containing silver. *J Therm Anal Calorim.* 2009;97:433-436.
47. Chen Y, Wei Y, Chang P, Ye L. Morphology-controlled synthesis of monodisperse silver spheres via a solvothermal method. *J Alloys Compd.* 2011;509:5381-5387.
48. Lin S, Ionescu C, Pike KJ, Smith ME, Jones JR. Nanostructure evolution and calcium distribution in sol-gel derived bioactive glass. *J Mater Chem.* 2009;19:1276-1282.

How to cite this article: Carta D, Jones JR, Lin S, Poologasundarampillai G, Newport RJ, Pickup DM. Neutron diffraction study of antibacterial bioactive calcium silicate sol-gel glasses containing silver. *Int J Appl Glass Sci.* 2017;8:364-371. <https://doi.org/10.1111/ijag.12318>